CLM-R246

CLM-R246

UKAEA

Report

THE STRUCTURE OF THE MAGNETIC EQUILIBRIUM IN THE HBTX1A REVERSED FIELD PINCH

D. BROTHERTON-RATCLIFFE
I. H. HUTCHINSON

CULHAM LABORATORY
Abingdon Oxfordshire
1984

C/18 Available from H. M. Stationery Office Price £5.00

CLM-R 246

THE STRUCTURE OF THE MAGNETIC EQUILIBRIUM IN THE HBTX1A REVERSED FIELD PINCH

D.Brotherton-Ratcliffe+, I.H.Hutchinson*

Culham Laboratory, Abingdon, Oxfordshire, U.K.

(Euratom/UKAEA Fusion Association)

ABSTRACT

The structure of the magnetic equilibrium in the Reversed Field Pinch HBTX1A has been measured using a magnetic probe inserted into the plasma. The picture revealed is one which agrees with a modified Bessel description of the field profiles. Variation of the measured flux-surface displacement with radius is consistent with that predicted by toroidal equilibrium theory. Profiles of the safety factor indicate that there is no pitch minimum. Pressure distributions are deduced which appear peaked on axis and are consistent with the measured values of the density and conductivity temperature. Values of $\beta_\theta \approx 14\%$ and $\langle\beta\rangle \approx 5\%$ are found, leading to an estimation of the energy confinement time of $\tau_E \approx 70\mu s$. Electric field profiles are presented from which a profile of effective parallel conductivity is calculated. This profile differs markedly from that estimated from the pressure profile using Spitzer conductivity, confirming the need for some type of dynamo mechanism and indicating its spatial form.

+ Royal Holloway college, London University, UK.

* Nuclear Engineering Department, MIT, Cambridge, Ma 02139, USA.

August 1984

ISBN 0 85311 130 8

1 INTRODUCTION

In order to understand the dynamics of plasma action in a contained plasma, it is essential to have a knowledge of the detailed structure of the long term (equilibrium) magnetic fields. In the Reversed Field Pinch (RFP) [1], where the poloidal and toroidal magnetic fields are of the same order, the most practical way of doing this is by employing insertable probes. The drawback of these probes is that they can affect the plasma.

Insertable magnetic probes have long been used in many thermonuclear containment devices, including Tokamaks (e.g. [2]). In RFP's they were extensively used on ZETA [3,4] and subsequently on fast programmed devices such as HBTX1 [5]. More recently they have been used in OHTE [6] and ETA–BETA II [7], where, for example, the measured field profiles were tested for linear stability and internal fluctuations studied.

In this paper we present measurements made with internal magnetic probes in the RFP HBTX1A at low currents. While essentially performing a similar analysis to the contemporary research referenced above, our studies concentrate in greater detail on equilibrium shift measurements, the pressure profile, and electric-field / conductivity measurements. Our analysis deals with the sustainment phase of the discharge where the greatest accuracy may be obtained in the calculated field profiles. As yet no systematic survey over different discharges has been carried out.

2 TECHNIQUES

The magnetic probe we have used is illustrated in figure 1. There are twenty-seven coils divided into nine sets of three. Each set of three comprises a radial, toroidal and poloidal coil, thus defining the magnetic field in nine equally spaced radial positions. The coils are set into a PTFE former which itself fits into a silica-glass sheath, 6mm in diameter. The

whole probe is attached to a bellows assembly which enables the tip of the probe to be positioned anywhere across the minor radius.

To obtain the most accurate estimate of the field profiles we average coil signals over both a limited time window and many shots. In this way we produce a mean magnetic field profile for a specific time range which is not affected by random fluctuations. We also move the probe over a limited distance so that slight misalignments of the individual coils tend to cancel out. In addition, the edge-field fit is improved by using external B_ϕ coils at the shell and a toroidal current Rogowski to provide extra points on the profiles. Even and odd polynomials are then fitted to B_ϕ and B_θ respectively (typically tenth order). The coefficients of these polynomials are altered in such a way as to correct for plasma displacement.

3 RESULTS

3.1 General

The evolution of the main discharge parameters and various probe signals for typical discharges are shown in figure 2. These shots are short (2 ms) decaying current discharges (100 kA) suitable for probe insertion. We present here results only from these type of discharges, although comparisons with discharges where the current is sustained reveal no obvious qualitative differences.

In figure 3 we plot the plasma current with the probe (a) retracted and (b) fully inserted. The main differences are that termination occurs about 7% earlier with the probe inserted and that the current decay rate is slightly increased. The effect of the probe on this plasma is thus rather small, an increase in resistivity of only about 20%, so we anticipate that the magnetic fields measured are representative of such discharges even without the probe inserted.

3.2 Magnetic Field And Current

Figure 4(a) shows 'raw' data from the probe plotted in profile form for a 0.2 ms time-slot in the middle of the sustainment phase (1.0-1.2 ms in figure 2) utilising a data-base of around 20 shots. The radial coordinate in this diagram refers to a vertical minor radius as the probe was inserted vertically. The scatter in points is due to shot to shot variation. The curve fitted to B_θ in this case includes a constant term as well as the odd powers of r in the polynomial expansion. However the least-squares fit is found to make this term very small so that the curve essentially intersects the origin. This shows that there is no vertical plasma shift.

In a toroidal system the plasma column will experience a horizontal shift due to curvature in the toroidal direction. Any radial field, which we measure with the probe, will give us information about this shift. Specifically, the shift, δ of the centre of the flux surface (assumed circular) passing through r, in relation to the geometrical axis is given by:

$$\delta = r\, B_r/B_\theta \ , \qquad - (1)$$

where r is the geometrical minor radius. We may compare this measured displacement with that predicted by formulae given by Shafranov for toroidal equilibrium [8]. In particular, the displacement of the flux surfaces Δ, as a function of radius r, is given by the following formula if we neglect plasma pressure (justified for this purpose since $\beta << 1$) and assume $a << R$:

$$\Delta(r) = \frac{1}{2R} \int_r^a \ell_i(r')r'\, dr' + \Delta_W(a) \qquad - (2)$$

where $$\Delta_W(a) = \frac{b^2}{2R} \{ \ln \left|\frac{b}{a}\right| + (1 - a^2/b^2)(\ell_i(a) - 1) \} \qquad - (3)$$

and $$\ell_i(r') = 2 \int_o^{r'} B_\theta^2(r)\, r\, dr \,/\, (r'\, B_\theta^2(r')). \qquad - (4)$$

Here a is the plasma minor radius, R the major radius of the torus and b, the minor radius of the shell. ℓ_i is the internal plasma inductance.

Figure 4(b) shows a comparison between this predicted displacement using the measured B_θ profile and that obtained from equation 1. The scatter in the displacement calculated by the latter method is rather large. This is mostly due to small alignment errors in the radial coils which then pick up the much stronger B_θ or B_ϕ fields. However, agreement is certainly reasonable showing that in the central region of the plasma the displacement is about 2.8 cm falling to around 1.7 cm at the limiters. The value of central displacement agrees well with that measured by X-ray emission profiles [9].

We may deduce from figure 4(b) that the plasma takes on the form of a uniformly shifted equilibrium in the central region of the discharge, since in this region the displacement appears approximately flat. Accordingly we may correct the field profiles so that we plot them, not as a function of the geometrical minor radius, but as a function of the radial coordinate whose origin is the shifted axis of the displaced flux-surfaces. Denoting the polynomial expansions of the two uncorrected field components as:

$$B_\theta(x) = \sum_{j=0}^{n} a_j x^{(2j+1)}; \quad B_\phi(x) = \sum_{j=0}^{n'} b_j x^{2j} \quad , \qquad - (5)$$

where x now represents the geometrical minor radius, the corrected field profiles may, in fact, be written (see appendix):

$$B_\theta(r) = \sum_{j=0}^{n} a_j \left(1 - \frac{j\Delta^2}{r^2}\right) r^{2j+1} \qquad - (6)$$

$$B_\phi(r) = \sum_{j=0}^{n'} b_j \left(1 - \frac{j\Delta^2}{r^2}\right) r^{2j} \quad ,$$

where Δ represents the central plasma displacement. These corrected profiles are shown in figure 5. In the outer regions, of course, they are

virtually indistinguishable from the uncorrected ones, as expected. However, near the axis there are substantial differences. In particular, inspection of figures 4(a) and 5 show that B_ϕ on axis is about 7 mT higher once the profiles have been corrected. While this may not be an enormous effect on the field profiles themselves, when estimating the pressure profile, this correction is very important.

Since we now have the field profiles as a function of the radial coordinate whose axis is the plasma axis, we may assume cylindrical symmetry in the derivation of quantities which depend on the fields. As we have noted above, this is due to the very constant form of the displacement as a function of radius in the inner region of the discharge (figure 4(b)). Hence, by differentiating the corrected field profiles according to the equation:

$$\underline{\text{Curl}}\ (\underline{B}) = \mu_o \underline{J}\ , \qquad - (7)$$

written in cylindrical coordinates, we may calculate the current density profiles. These are shown in figure 6. The accuracy in the outer regions of the discharge is not sufficient to distinguish whether the toroidal current density reverses as expected from certain force-free models.

Figure 7 shows profiles of the parallel and perpendicular current densities $\underline{J}.\underline{B}/B^2$ and $\underline{J}x\underline{B}/B^2$. To a good approximation we see that the discharge is force-free. In fact, by inspection of this figure, the ratio $J_{//}/J_{\perp}$ may be seen never to be less than about 10 and in the central region of the discharge around 50. Within errors the μ ($= \underline{J}.\underline{B}/B^2$) profile is flat from the axis out to about 15 cm where it falls monotically to zero at the wall. Accordingly we can deduce that the profiles which we observe are in good agreement with a modified essel description (MBFM) [10].

Figure 8 shows a profile of the safety factor $q = rB_z/RB_\theta$ which appears monotonic. This observation excludes the presence of instabilities driven by 'pitch minima'. The value of q on axis is about 0.2, signifying that resonant m = 1 instabilities in the inner region of the plasma must have a

toroidal mode number greater than $|n| \approx 5$. This agrees with recent measurements of the fluctuation activity on HBTX1A [11]. Lastly the value of q at the limiters is about -0.04. In a similar fashion this imposes a lower limit on the toroidal mode number of $|n| \approx 25$ for m = 1 modes to be resonant outside the reversal surface.

3.3 Estimation Of The Pressure Profile

By integrating the equilibrium pressure balance equation:

$$\underline{\text{Grad}}\ (P) = \underline{J} \times \underline{B} \qquad - (8)$$

in cylindrical form from the limiters inwards it is possible to obtain the pressure profile. It must be stressed that the computation of this profile is extremely sensitive to experimental errors and is thus very uncertain with low β values. This is because the pressure profile is directly related to the perpendicular current density which in our case is very small. However, with the type of corrections we have applied to our estimates of the field profiles, we find that we can estimate the pressure profile with useful accuracy in the sustainment phase of the discharge. In particular, this is because we can improve the edge-field fit in this period by using external coils to weight a vacuum-field configuration from the limiters outwards. This is accomplished by including extra points, calculated from the external coils, with a '1/r' dependence for B_θ and a constant value for B_ϕ. This process improves not only the edge-field fit, but also the central region fit as it allows higher order polynomials to be fitted to the data without introducing spurious oscillations at the edge. In addition to this, an equally important factor is the correction we have made to the field profiles to take into account plasma displacement. Without this, we would expect false features to appear on the pressure profile near the axis. Lastly, and not by any means least important, is the fact that our probe

perturbs the plasma only very slightly.

Figure 9 shows a best estimate of the pressure profile obtained by averaging over several polynomial fits for each of many different random realisations of the initial data. The error bar shown in this graph pertains to the on-axis pressure and is calculated as the standard deviation over the many polynomial fits and random realisations and decreases monotonically to zero at the limiters, where we assume that the wall pressure is zero. The profile may be characterised by the following values of the various β parameters:

$$\beta_\theta = \frac{2\mu_o \langle P \rangle}{B_\theta(a)^2} \approx 14\% \pm 5\% \qquad - (9)$$

$$\langle \beta \rangle = \frac{2\mu_o \langle P \rangle}{\langle B^2 \rangle} \approx 5\% \pm 2\% \qquad - (10)$$

$$\beta_o = \frac{2\mu_o P(0)}{B(0)^2} \approx 9\% \pm 3\% , \qquad - (11)$$

where a represents the plasma radius.

The overall shape of the best estimate pressure profile is peaked on axis. At the extreme of the error estimate the profile could be flat (or slightly hollow) out to about 8 cm but not beyond.

In the sustainment phase of the discharge we find that the pressure profile is essentially constant in shape and evolves in magnitude so as to keep β approximately constant. During periods of the discharge when the plasma current varies very quickly, the termination and set-up phases, it is not generally possible to use edge coil measurements to improve the fitting procedure owing to inductive effects in the liner. So any study of the evolution of the pressure profile will inherently be subject to much greater inaccuracy. Despite this, however, we are able to say that in the time-interval just before termination the pressure peaks on axis (increasing by a factor of about 1.5 in absolute magnitude) indicating that the plasma undergoes a sharp compression before extinction.

3.4 Electric Field and Energy Confinement

In the approximation of cylindrical symmetry the Faraday equation:

$$\underline{\text{Curl}}\ (\underline{E}) = -d\underline{B}/dt \qquad - (12)$$

defines the toroidal and poloidal electric field distributions as a function of minor radius given suitable boundary conditions at the wall, which are provided by loop voltage measurements. Typical profiles, obtained by subtracting successive estimates of the field profiles, are shown in figure 10.

Since we have the plasma kinetic energy from our pressure measurements and the ohmic dissipation power from $\underline{E}$ and $\underline{J}$ we may obtain the energy confinement time as:

$$\tau_E = \iiint_{V_{plasma}} \frac{3}{2} P \, dV \; / \; \iiint_{V_{tot}} \underline{E}.\underline{J} \, dV \ , \qquad - (13)$$

where we have ignored dP/dt since it is small in our case compared to $\underline{E}.\underline{J}$. Our measurements yield a value of $\tau_E = 70\mu s$ in which the uncertainty is virtually all in the pressure and so is about 30% as with $\langle\beta\rangle$.

3.5 Conductivity

Since we have profiles of $\underline{E}$ and $\underline{J}$ we can obtain profiles of an effective parallel conductivity defined as:

$$\sigma_{eff} \equiv (\underline{J}.\underline{B})/(\underline{E}.\underline{B}). \qquad - (14)$$

This is shown in figure 11. Now if the plasma obeyed a simple Ohm's law of the form:

$$\underline{\underline{\sigma}}.(\underline{E} + \underline{v}\times\underline{B}) = \underline{J} \qquad - (15)$$

(which it does not) then naturally σ_{eff} would be equal to the actual (Spitzer) conductivity $\sigma_{//}$.

The true conductivity $\sigma_{//}$ may be obtained directly from an estimate of the electron temperature profile. We may derive this crudely by assuming that the electron and ion temperatures are equal and that the shape of the density profile is the same as the electron temperature so that $T_e \propto P^{1/2}$. Then, using the Spitzer formula [12] for the conductivity with an assumed constant resistivity anomaly Z, we can find the conductivity σ_T corresponding to the electron temperature profile deduced. This is shown in figure 11 for Z = 2 and 4.

The current-to-field ratio σ_{eff} has a clearly hollow profile even in these decaying-current discharges whereas the Spitzer estimate, σ_T, is naturally peaked on axis because the temperature profile we deduce is monotonically decreasing. Plausibly, one could argue that virtually any T_e profile would become monotonic because of thermal deposition and the transport equations regardless of our somewhat cavalier assumptions about the density profiles.

It seems most unlikely that the discrepancy between σ_{eff} and σ_T could be explained by spatial variations of Z since this would require $Z < 1$ at the edge. We conclude, as noted above, that the plasma does not satisfy the simple Ohm's law of equation 15 but experiences some type of 'dynamo effect' sustaining the reversal [13].

4 DISCUSSION

That the flux-surface shift deduced from B_r is consistent with the Shafranov value is hardly surprising. The important point is that, once measured, the shift can be properly corrected for in further analysis of the measurements from the viewpoint of the cylindrical approximation. Without proper correction serious errors could occur.

The μ profile of parallel current confirms the observations elsewhere [6,7] and also the theoretical expectation that the central regions of the RFP relax to the minimum energy, μ = constant, state but that $\mu \to 0$ at the wall. It thus supports the modified Bessel function model as a reasonable approximation to RFP profiles.

The absence of a 'pitch minimum' in the outer regions of the discharge is an interesting result. As well as excluding the instabilities driven by such a configuration it also confirms the rationale for choosing the RFP over 'unreversed' pinches.

The deduction of pressure profiles from magnetic probe measurements is, as we have seen, subject to considerable uncertainty owing to the accumulation of calibration, alignment and other errors. Nevertheless we believe that the profile presented represents a reasonable approximation to the actual profile. In confirmation of this we note that, at this time in the discharge, interferometer measurements show that the chord averaged electron density is about 2.7×10^{19} m^{-3}. Assuming a parabolic distribution for which $n_{eo} = 3\langle n_e \rangle/2$, taking the central electron temperature to be twice the mean conductivity temperature (as indicated by Thompson scattering for different discharges [14]), T_e = 50 eV, and taking $T_e = T_i$ and $n_e = n_i$ gives an independent rough estimate of the central beta of 0.064. This then agrees quite well with the value 0.09 in figure 9, considering the uncertainties in the assumption that $T_e = T_i$, of the assumed n_o and T_{eo}, and P_o.

The accuracy we estimate for P(r) enables us to rule out the possibility that the pressure profile is rather flat out to a radius close to the reversal surface and then steeply falling from there to the wall. The importance of this observation is in excluding certain radial dependences of the transport coefficients. For example, recent measurements [11] on HBTX1A indicated that the magnetic field lines inside the reversal surface were stochastic and the transport associated with such stochasticity was

sufficient to explain the energy losses observed. Those measurements were insufficient to establish whether or not the field was stochastic at the reversal surface and beyond. This is an important point since recent 3D-MHD simulations [15] indicate that even if the centre of the RFP is stochastic, the edge region, from about the reversal surface outward, may have well defined magnetic flux surfaces and hence much smaller diffusivity.

If such a situation of good 'edge confinement' were to occur then the temperature would, in order to satisfy the diffusion equations, adopt a profile flat in the centre, where the electron diffusivity is large, and steep at the reversal surface and beyond, where it is small. Less obviously the density profile might also be expected to take on this form and and in this case the pressure profile would follow suite. However, this is precisely the profile shape which is ruled out by our measurements.

Of course, in the absence of actual ambipolar stochastic transport calculations, the assumption that the density profile must follow the temperature profile is weak and thus our measurements cannot fully rule out the existence of a stochastic interior and non-stochastic edge. However, if we do assume that the plasma is only stochastic inside the reversal surface, then the density profile consistent with our measurements will have to be very peaked.

Our measurements of σ_{eff} and their deviation from the expected profile shape of the ohmic conductivity are a rather direct observation of the 'dynamo mechanism' at work, even in decaying discharges. Of course, in steady state discharges the persistence of magnetic field reversal is itself a manifestation of this reversal sustaining mechanism. Unfortunately, the measurements do not presently enable us to distinguish between the various possible detailed mechanisms which may be responsible for the 'dynamo' effect (for example, the mean-field electrodynamics approach [16,17], the tangled discharge model [18] or some form of non-local resistivity due to stochasticity). Further theoretical refinement

of these models in the future may reveal characteristics which are sufficiently well defined as to be testable against our present results.

5 CONCLUSIONS

We have presented results obtained from the insertion of a magnetic probe into the RFP HBTX1A. The effect of the probe on the plasma is to increase the resistance by only about 20% and therefore we have assumed that the measurements have a direct relevance to discharges where the probe is not inserted. The magnetic field profiles obtained agree well with an MBFM description. Measurements of horizontal plasma displacement as a function of radius agree, within uncertainty, with the predicted theoretical variation according to Shafranov. In particular the value of displacement in the centre of the discharge is 2.8 cm falling to about 1.7 cm at the limiters. No vertical plasma shift is observed.

Examination of the pitch profile reveals that there are no pitch minima and that $m = 1$ modes with $|n| < 5$ in the core or $|n| < 25$ at the edge, if present, would be non-resonant.

Significant emphasis has been placed in this study on the accurate determination of the pressure profile. Results are consistent within errors with independent values of the temperature and electron density. We find that typically $\beta_\theta \approx 14\%$, $\langle\beta\rangle \approx 5\%$ and $\beta_o \approx 9\%$. The profile of pressure is peaked on axis and therefore it appears unlikely that the plasma experiences significantly lower diffusivity at the reversal surface (and beyond) than in the central regions. Electric field profiles have been calculated and have then been used to give an effective parallel conductivity which has been compared to that calculated from the pressure profile, assuming a suitable density profile. The very great difference between these two estimates requires the presence of some kind of a dynamo mechanism acting in such a way as to sustain field reversal.

6 ACKOWLEDGEMENTS

The authors would like to thank Dr H.A.Bodin for his many helpful comments concerning the manuscript.

REFERENCES

/1/ Bodin H A B , Newton A A: Nucl Fusion 20, p 1255 (1980).

/2/ e.g. Hutchinson I H ,Morton A H: Nucl Fusion 16 p 477 (1976).

/3/ Rusbridge M G , Lees D J and Saunders P A H : Nucl Fusion Suppl. pt 3, 895 (1962).

/4/ Rusbridge M G , Jones H W , Lees D J , Saunders P A H and Witalis E A : Plasma Phys. 3, 98 (1961).

/5/ Gowers C W ,Robinson D C ,Sykes A ,Verhage A J L Wesson J A Watts M R C ,Bodin H A B in Plasma Physics and controlled nuclear fusion research (Proc.6th Int. conf. Berchtesgaden, 1976) Vol 1, IAEA Vienna (1977) 429.

/6/ La Haye R J, Carlstrom T N ,Goforth R R , Jackson G L , Schaffer M J , Tomano T , Taylor P L : General Atomic report GA-A16945 and submitted to Nucl Fusion.

/7/ Antoni V and Ortolani S: Plasma Physics 25 799 (1983).

/8/ Shafranov V D in Reviews of Plasma Physics 2 p130 Ed Leontovich M A Consultants Bureau New York.

/9/ Malacarne,M.,Hutchinson,I.H.,Brotherton-Ratcliffe,D. in Proc. Varenna conf. (Italy) 1983.

/10/ Whiteman K J : Plasma Phys. 7 (1965) 293.

/11/ Hutchinson I H , Malacarne M , Noonan P , Brotherton-Ratcliffe D : Nucl Fusion 24 (1984) 59.

/12/ Spitzer L : 'Physics Of Fully Ionised Gases', Interscience tracts on Physics and Astronomy, Interscience Publishers, John Wiley and sons, New York / London.

/13/ e.g. Moffet H K : 'Magnetic Field Generation In Electrically Conducting Fluids', Cambridge niversity ress (1978).

/14/ Bodin H A B , Bunting C A , Carolin P G , Guidicotti L , Gowers C W , Hirano Y , Hutchinson I H , Jones P A , Lamb C , Malacarne M , Newton A A , Piotrowicz V A , Shimada T, Watts M R C in Plasma Physics And Controlled Nuclear Fusion Research Proc. conf. Baltimore, 1982, Vol 1, IAEA Vienna 1983 pp641-657.

/15/ Schnack D D, Caramana E J, Nebel R A : Bulletin of APS 28 (1983) 8 p1229.

/16/ Gimblett C G , Watkins M L in controlled Fusion and Plasma Physics (proc. 7th Europ. conf. Lausanne,1975) Vol.1. (1975) 103.

/17/ Gimblett C G , Watkins M L in Pulsed High β Plasmas (Proc. 3th op. Conf. Abingdon, 1975) Permagon Press, London (1976) 279.

/18/ Rusbridge M G : Plasma Phys. 19 (1977) 499.

APPENDIX

CORRECTION OF THE FIELD PROFILES FOR A UNIFORM HORIZONTAL PLASMA SHIFT

We have seen that, in the central region of the discharge, the plasma equilibrium may be characterised by a set of concentric magnetic surfaces whose centre is shifted a distance Δ from the geometrical minor axis (GMA). Figure A1 shows the situation. Our probe is inserted vertically to the GMA, the individual coils measuring $B_{mx}(y)$, $B_{my}(y)$ and $B_{mz}(y)$. The problem we address is to determine the true poloidal and toroidal fields $B_\omega(\rho)$ and $B_z(\rho)$.

A.1 Toroidal Field

By definition we may write

$$B_{mz}(y) = B_z(\rho) = B_z(\sqrt{[y^2 + \Delta^2]}). \qquad - (A1)$$

And so, on expansion, this yields

$$B_z(\rho) \approx B_z\left(y + \frac{\Delta^2}{2y}\right) \approx B_z(y) + \frac{\Delta^2}{2y}\,\frac{dB_z}{d\rho}, \qquad - (A2)$$

which is valid provided $\Delta^2/y^2 << 1$. Using A1 again this may be recast in the following form

$$B_z(y) \approx B_{mz}(y) - \frac{\Delta^2}{2y}\,\frac{dB_{mz}}{dy} \quad . \qquad - (A3)$$

Obviously, near the axis this formula is not justified. However, in this region we may expand in the following manner :

$$B_z(\rho) \approx B_z(0) + \frac{\rho^2}{2}\frac{d^2B_z}{d\rho^2}\bigg|_{\rho=0} \qquad - (A4)$$

$$\approx B_z(y) + \frac{\Delta^2}{2}\frac{d^2B_{mz}}{dy^2}\bigg|_0 \quad , \qquad - (A5)$$

provided $\left|\frac{\Delta^3}{6B_{mz}} \cdot \frac{d^3B_{mz}}{dy^3}\right| << 1.$ - (A6)

Now since near the axis $\left.\frac{d^2 B_{mz}}{dy^2}\right|_0 \approx \left.\frac{1}{y}\frac{dB_{mz}}{dy}\right|_y$ we again obtain equation A3.

So this equation in fact holds subject to the condition A6 which is not difficult to satisfy. Our correction scheme for B_z is therefore to use

$$B_z(y) = B_{mz}(y) - \frac{\Delta^2}{2y}\frac{dB_{mz}}{dy} \quad . \qquad - (A7)$$

Hence if we expand the measured field as an even polynomial in y so that

$$B_{mz}(y) = \sum_{j=0}^{N} b_j\, y^{2j} \qquad - (A8)$$

the corrected toroidal field may be written

$$B_z(y) = \sum_{j=0}^{N} b_j \left(1 - \frac{j\Delta^2}{y^2}\right) y^{2j} \quad . \qquad - (A9)$$

A.2 Poloidal Field

A similar analysis to that above may be carried out on the poloidal field component by expanding this time for $B_\omega(\rho)/\rho = B_{mx}/y$. As before, in both the inner and outer regions of the discharge we are led to the following correction formula :

$$B_\omega(y) = B_{mx}(y) - \frac{\Delta^2}{2}\frac{d}{dy}\left(\frac{B_{mx}}{y}\right) \quad . \qquad - (A10)$$

Thus, if we expand B_{mx} as an odd polynomial series so

$$B_{mx}(y) = \sum_{j=0}^{N} a_j y^{(2j+1)} \qquad - (A11)$$

then the true poloidal field is given by

$$B_\omega(y) = \sum_{j=0}^{N} \left(1 - \frac{j\Delta^2}{y^2}\right) y^{(2j+1)} \qquad - (A12)$$

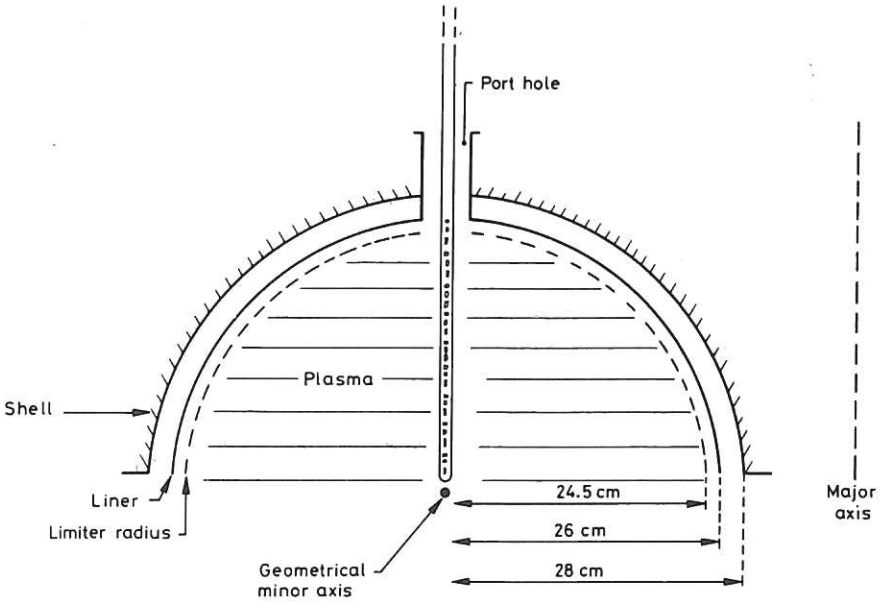

Fig. 1 Illustration of the magnetic probe.

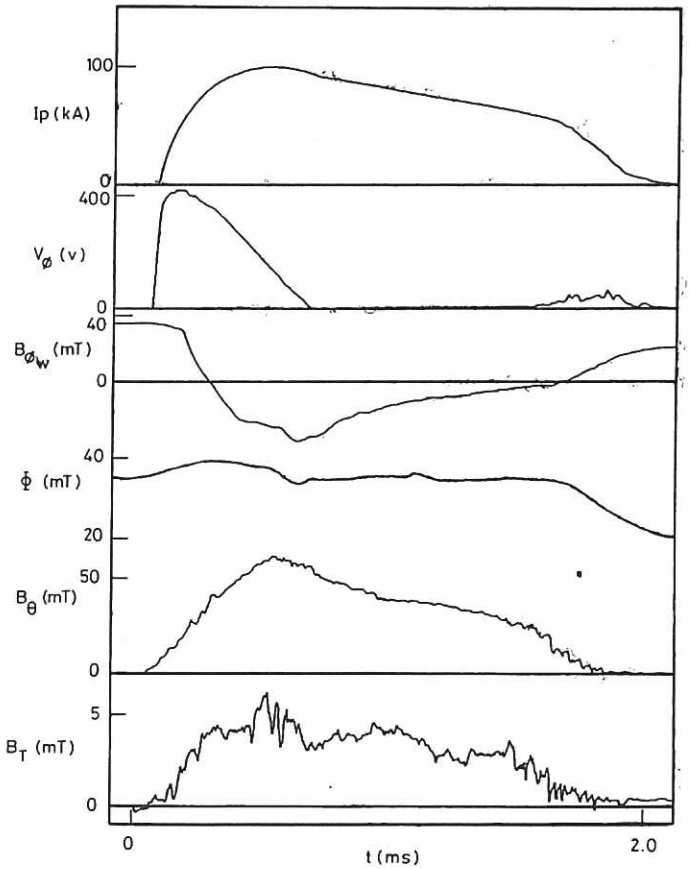

Fig. 2 Typical parameter traces: Toroidal current (I_p), loop voltage (V_ϕ), toroidal field at wall ($B_{\phi w}$), toroidal flux (Φ), B_θ probe trace ($B_\theta{}^p$) and B_r probe trace ($B_r{}^p$).

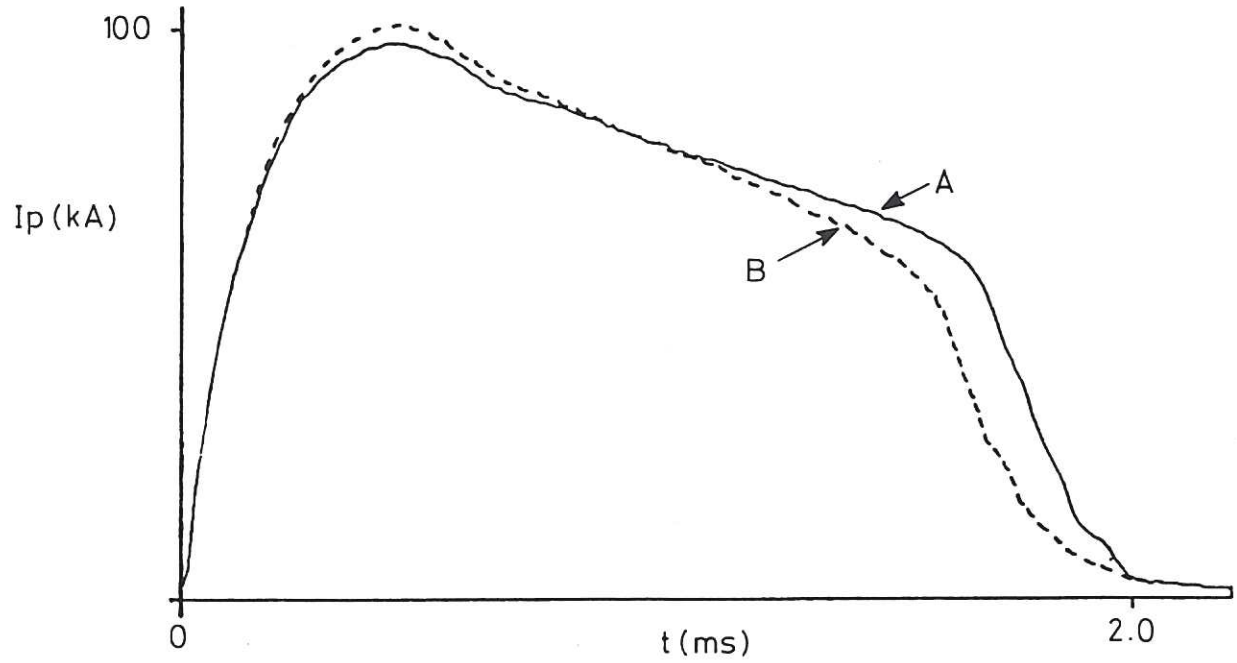

Fig. 3 Toroidal plasma current with probe retracted (a) and probe inserted (b).

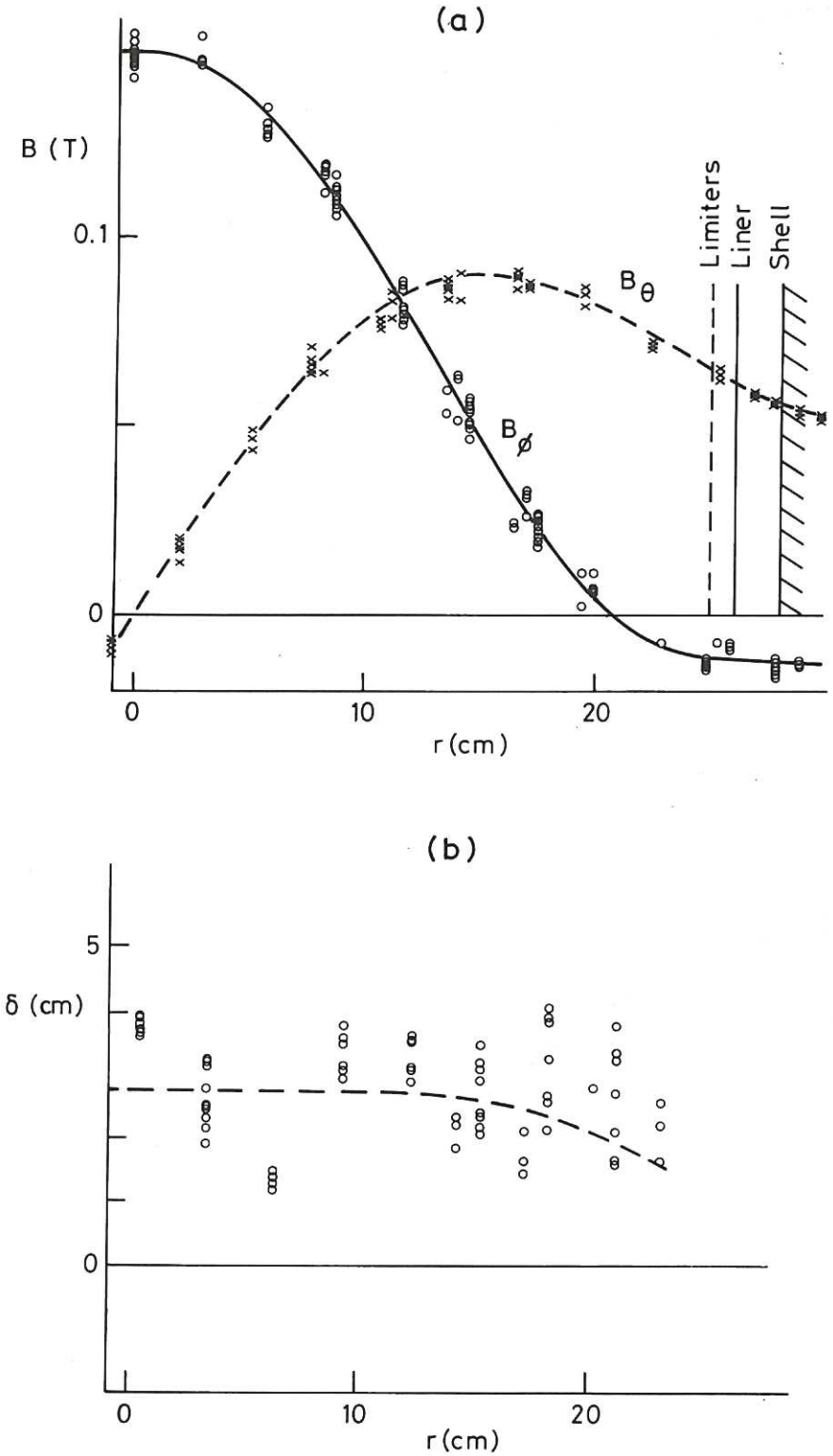

Fig.4 (a) 'Raw' magnetic field profiles and (b) measured plasma displacement vs radius compared with theoretical displacement calculated from the field profiles.

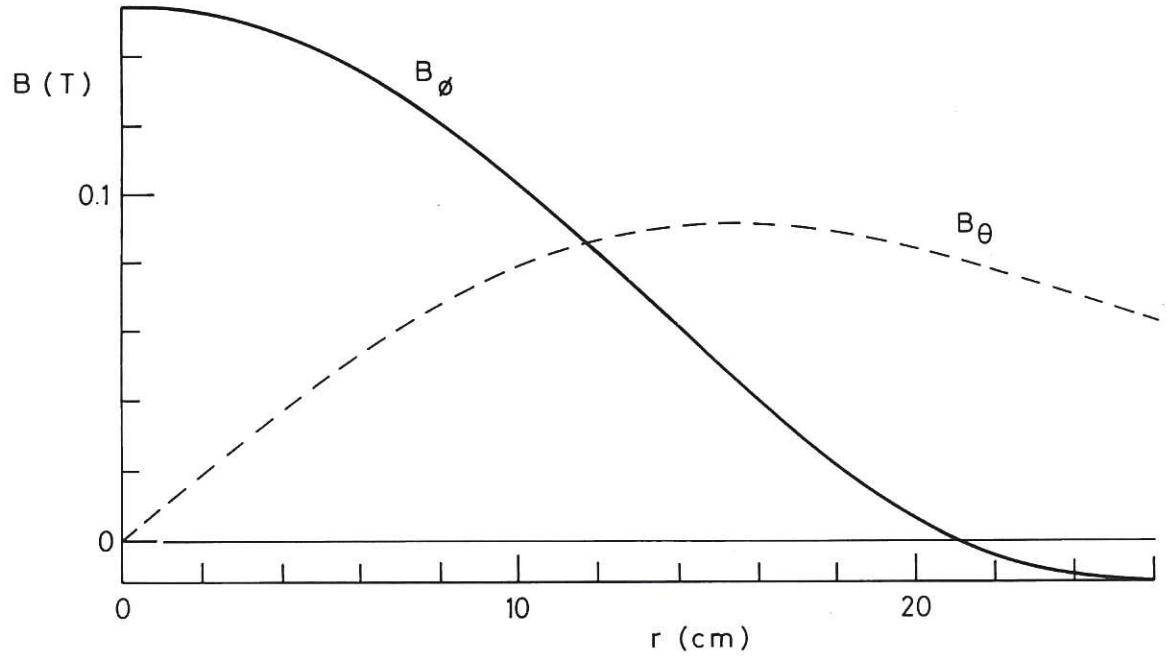

Fig.5 Shift-corrected magnetic field profiles.

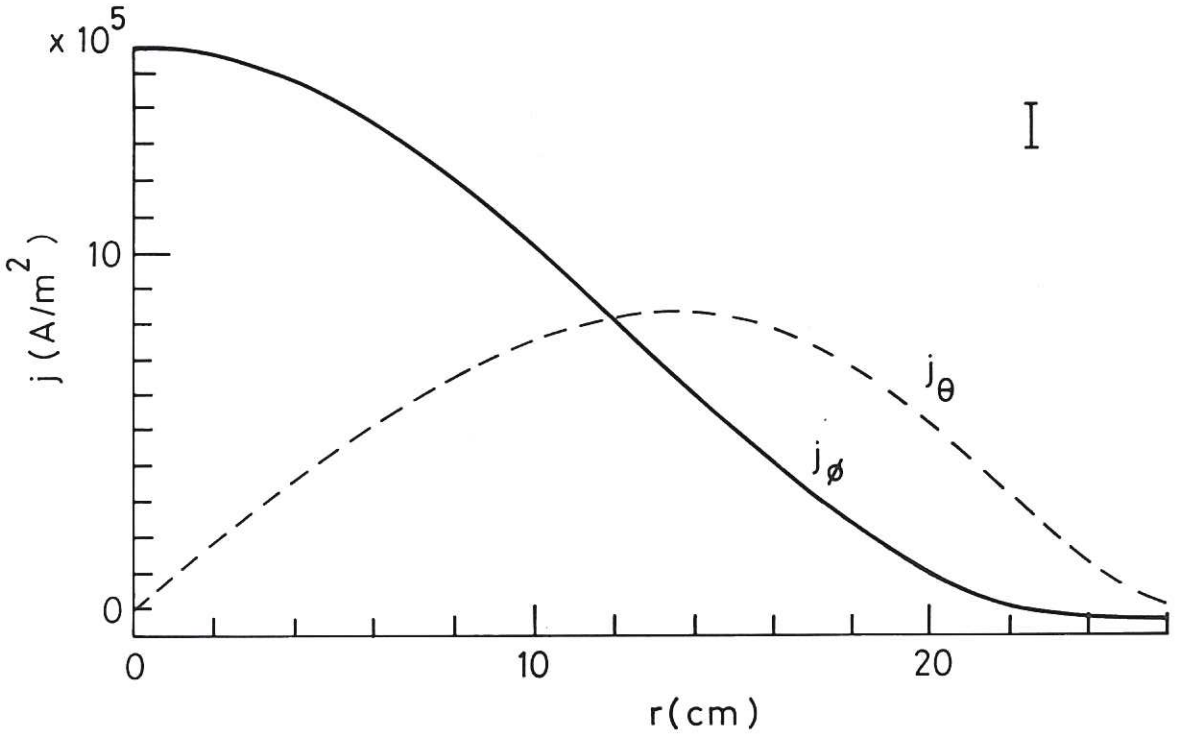

Fig.6 Current profiles J_θ and J_ϕ.

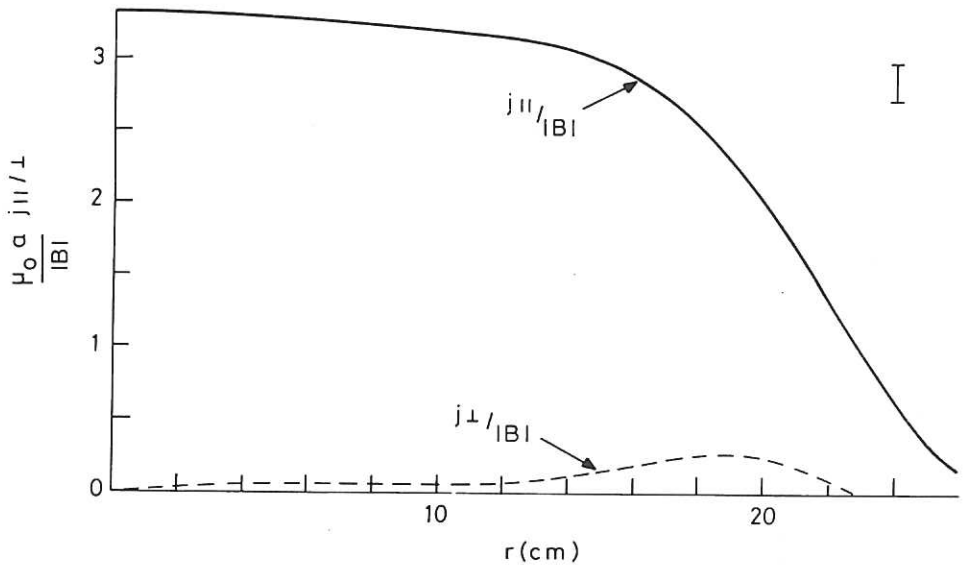

Fig. 7 Profiles of parallel and perpendicular current densities, $\underline{J}.\underline{B}/B^2$ and $|\underline{J} \times \underline{B}|/B^2$.

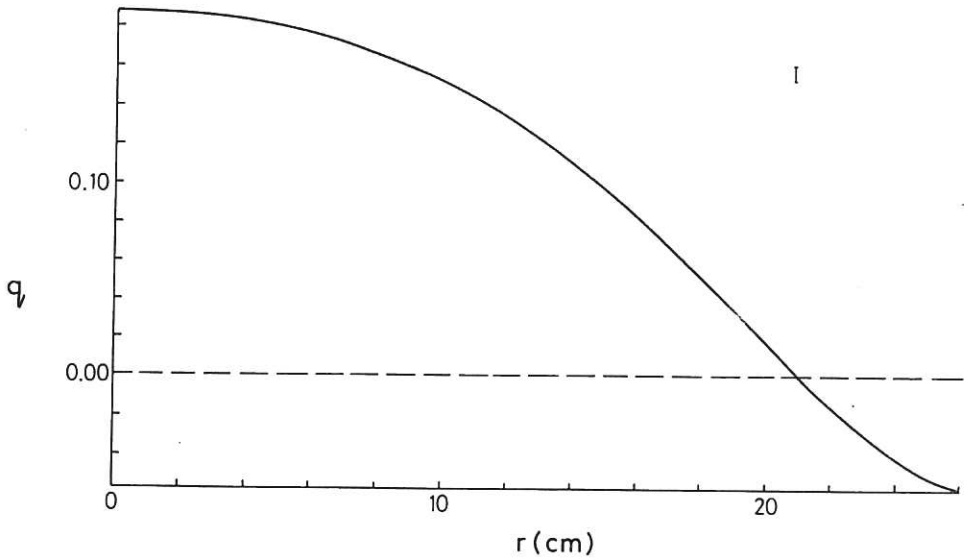

Fig. 8 Profile of the safety factor $q = rB_{\phi}/RB_{\theta}$.

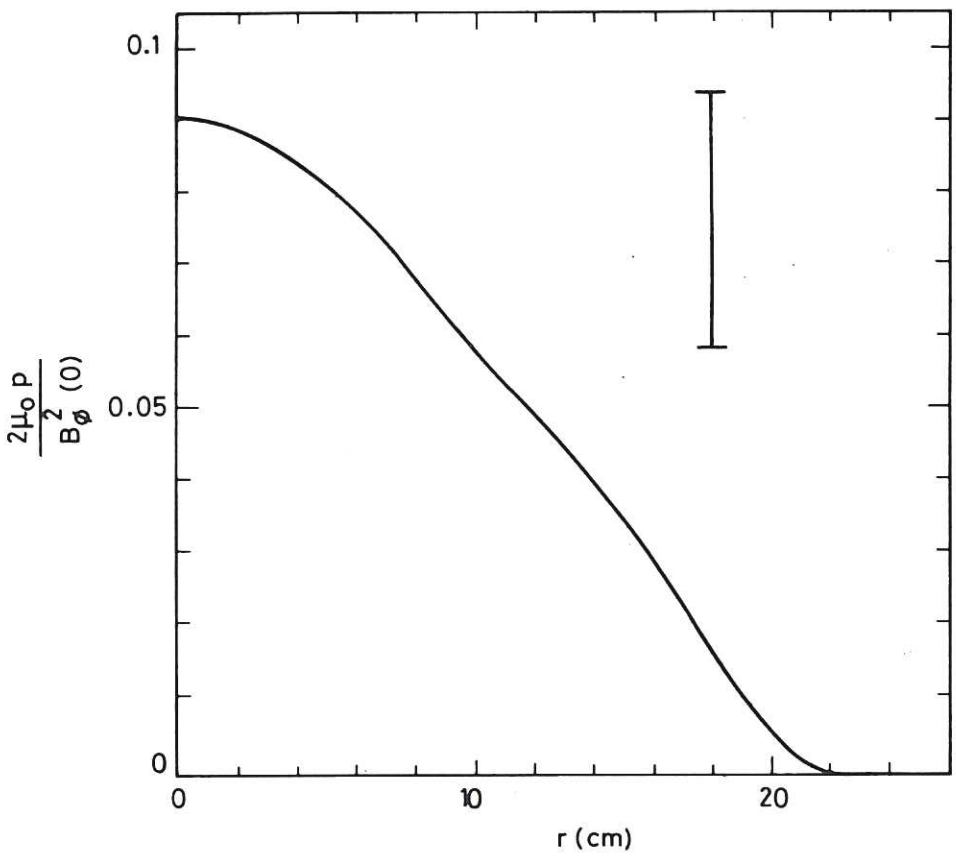

Fig.9 Profile of kinetic pressure normalised to the on-axis magnetic pressure.

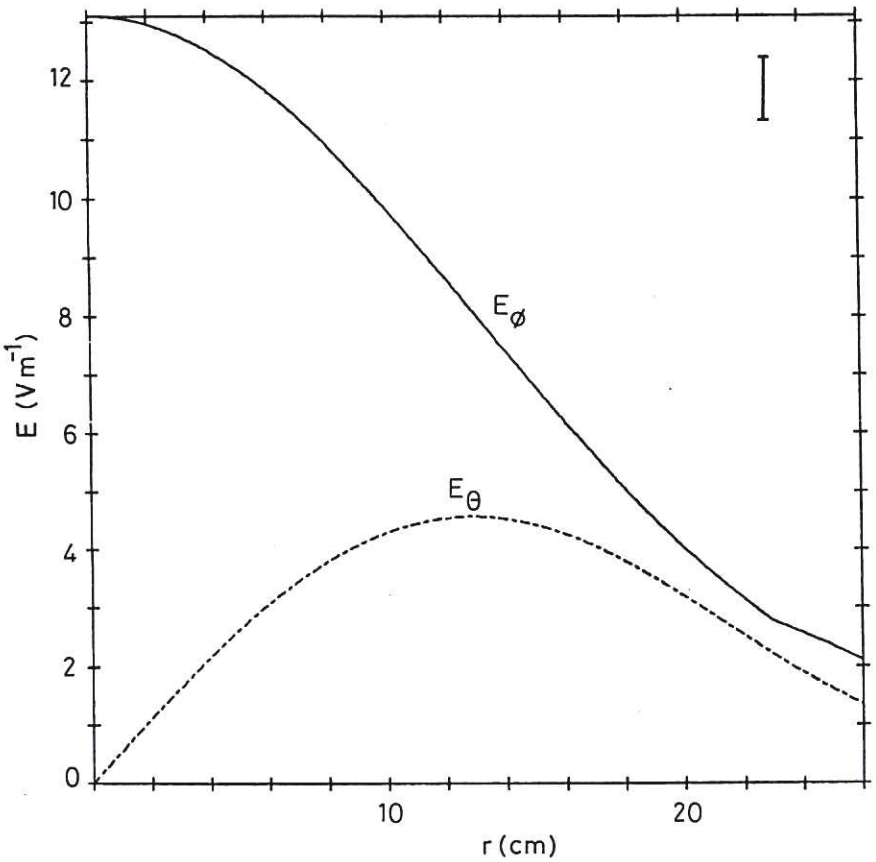

Fig.10 Electric field profiles E_θ and E_ϕ.

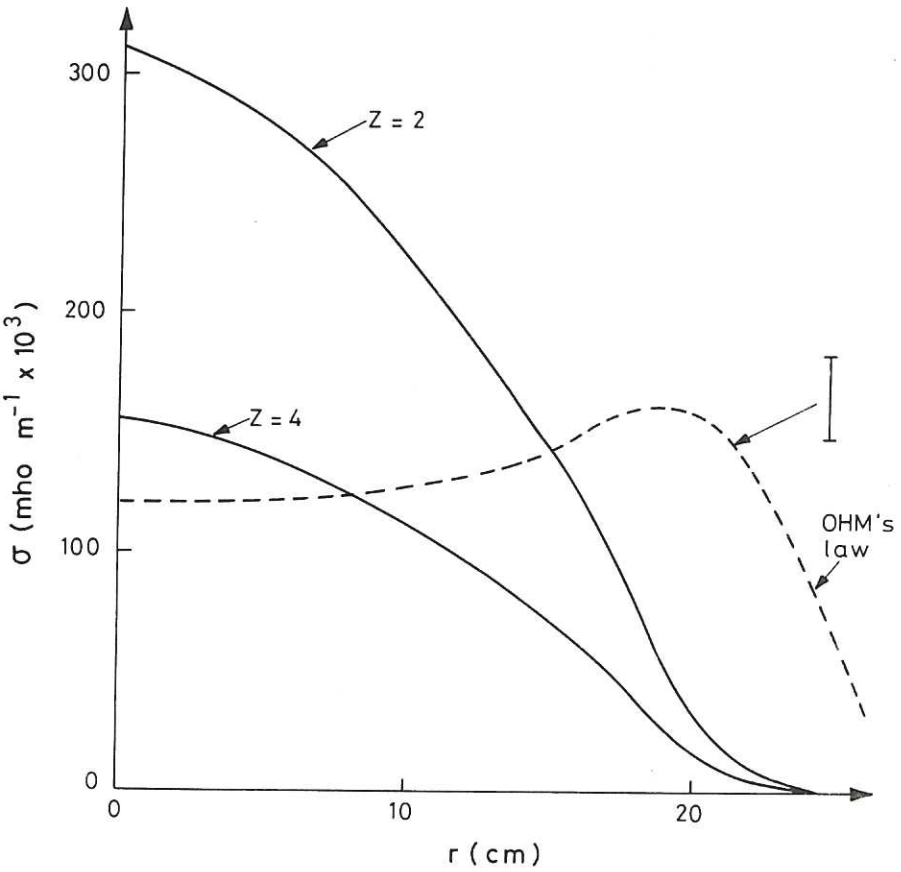

Fig. 11 Profile of $\sigma_{eff} = (\underline{J}.\underline{B})/(\underline{E}.\underline{B})$ compared with several profiles estimated from the pressure for Z = 2,4.

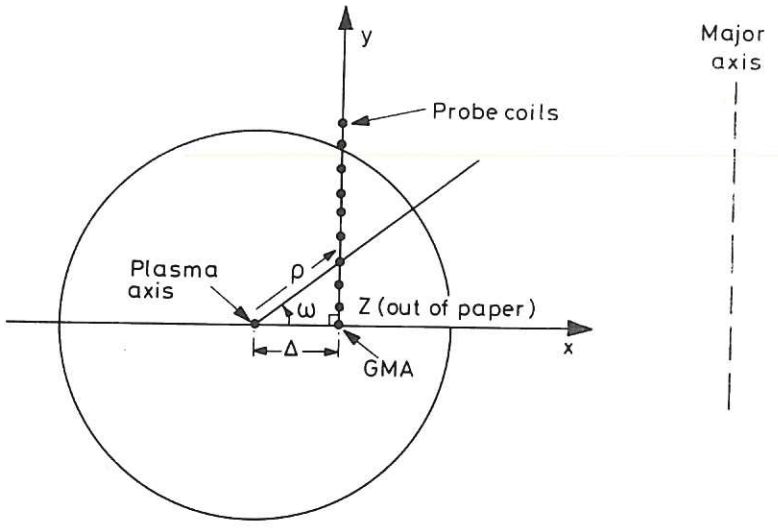

Fig. A1 Diagram showing the shifted plasma equilibrium. The point $\rho = 0$ represents the centre of symmetry of the innermost flux surface and the point marked GMA represents the geometrical minor axis.

HER MAJESTY'S STATIONERY OFFICE

Government Bookshops

49 High Holborn, London WC1V 6HB
(London post orders: PO Box 276, London SW8 5DT)
13a Castle Street, Edinburgh EH2 3AR
Brazennose Street, Manchester M60 8AS
Southey House, Wine Street, Bristol BS1 2BQ
258 Broad Street, Birmingham B1 2HE
80 Chichester Street, Belfast BT1 4JY

Publications may also be ordered through any bookseller